Letter

Glassy electrons at the first-order Mott metal-insulator transition

Shreya Kumbhakar,[1,*] Saurav Islam,[1,†] Zhiqiang Mao,[2] Yu Wang,[2] and Arindam Ghosh[1,3]
[1]*Department of Physics, Indian Institute of Science, Bangalore 560012, India*
[2]*Department of Physics, Pennsylvania State University, University Park, Pennsylvania 16802, USA*
[3]*Centre for Nano Science and Engineering, Indian Institute of Science, Bangalore 560012, India*

(Received 10 May 2022; revised 16 August 2022; accepted 10 November 2022; published 23 November 2022; corrected 2 December 2022)

The Mott metal-insulator transition remains one of the most scrutinized concepts in condensed matter physics. However, the kinetics of the charge carriers at the transition, involving both orbital and spin degrees of freedom, still remains poorly understood. A perfect platform to distinguish between the role of such competing interactions is strongly correlated oxides offering rich phase diagrams, which we use here to address the electron kinetics at the transition. We show a critical slowing down of the electron kinetics at the first-order Mott metal-insulator transition in the Ruddlesden-Popper oxide $Ca_3(Ru_{0.9}Ti_{0.1})_2O_7$ using low-frequency noise in resistance fluctuations. A critical slowing down of the electron kinetics is manifested as an enhancement of noise by an order of magnitude at the transition with a large shift of the spectral weight to lower frequencies. The second spectrum of noise is frequency dependent, indicating the presence of correlated fluctuations which get suppressed under the application of a magnetic field. Our experiments provide compelling evidence of the formation of a spin-glass phase at the transition in these systems.

DOI: 10.1103/PhysRevB.106.L201112

Despite immense theoretical and experimental progress, the metal-insulator transition (MIT) [1–3] still remains an active area of research [4–13]. These transitions can be driven by disorder, leading to Anderson insulators [14] or strong correlation leading to Mott insulators [1,2,15]. Mott insulators are particularly important because of potential applications in diverse fields due to the tunability of the phase transition with external parameters [10–12]. In real materials, however, the complex interplay of lattice, spin, and orbital degrees of freedom makes the critical phenomena at Mott transition a matter of active discourse [16–19]. An issue of fundamental interest is the electronic kinetics and the presence of glassy behavior at the transition [20]. Although the slowing down of electron kinetics is generally predicted for second-order phase transitions, a general consensus regarding the nature of critical fluctuations near the first-order Mott transition is lacking. Here, we address these questions with a very careful set of measurements, in a carefully chosen material with a high transition temperature, where quantum interference/localization effects do not dominate. A critical slowing down of electrons has been observed in organic salts [21] at temperature $T \approx 34$ K, but its nature in a crystalline solid where both orbital and spin degrees of freedom have competing strengths is not known. Experiments involving three-dimensional (3D) doped semiconductors [22], disordered oxide films, 2D electron gases in metal-oxide-semiconductor field-effect transistors (MOSFETs) [23], etc., have also claimed glassy electron kinetics at the transition, but most of them were carried out at low temperature where localization effects due to quantum interference were also rather strong. Additionally, the electron kinetics at Mott transitions at high temperatures, for example, in the perovskite class of oxide films or rare-earth nickelates [24–26], becomes difficult to explore due to emergent spatial inhomogeneity at the transition.

The Ruddlesden-Popper (RP) ruthenate $Ca_3(Ru_{0.9}Ti_{0.1})_2O_7$ [27] is an excellent platform to understand the generality of electron kinetics at the Mott transition, where one can attempt to distinguish between the roles of orbital and spin degrees of freedom close to the critical temperature, which can be as high as ≈110 K. RP-type ruthenates [28] are a natural playground to observe rich correlated behavior, where physical parameters such as doping, temperature, pressure, and electric field affect the distortion of RuO_6 octahedra, leading to drastic changes in the magnetic and electrical properties of the system. Recent work in such compounds has reported spin-triplet superconductivity in Sr_2RuO_4 [29,30], a field-tuned nematic electronic phase [31], itinerant ferromagnetism [32,33], an antiferromagnetic (AFM) Mott insulating state [34], and paramagnetic bad metallicity [35]. $Ca_3Ru_2O_7$ is a RP-type compound, which undergoes two phase transitions [36,37], a Néel transition from the metallic paramagnetic (PM) phase at high temperature (T) to a metallic a-AFM phase below $T = 56$ K and a structural phase transition to a b-AFM phase below $T = 48$ K, where the in-plane resistivity increases and the spin orientation switches from the a axis to the b axis. Isovalent Ti doping into the Ru sites disrupts the hopping of carriers in $Ca_3(Ru_{1-x}Ti_x)_2O_7$ and results in a bandwidth-controlled Mott transition from a metallic PM phase to an insulating G-AFM phase for $x > 0.05$ [27,38]. However, within a narrow range of magnetic field (B) and T, a stripelike metallic domain has been observed in $Ca_3(Ru_{0.9}Ti_{0.1})_2O_7$ [39], which is believed to be the a/b-AFM

*Corresponding author: shreyak@iisc.ac.in
†Corresponding author: ski5160@psu.edu. Present address: Department of Physics, Pennsylvania State University, University Park, Pennsylvania 16802, USA.

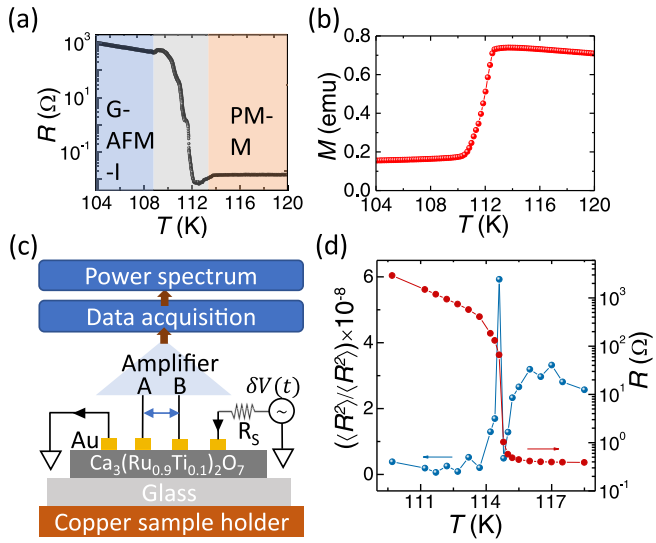

FIG. 1. Characterization of $Ca_3(Ru_{0.9}Ti_{0.1})_2O_7$. (a) Resistance ($R$) vs temperature ($T$) showing the metal (M) to insulator (I) transition at $T \approx 112$ K. Blue and red regions indicate insulating G-antiferromagnetic (G-AFM-I) and metallic paramagnetic phases (PM-M), respectively. (b) Magnetization (M) vs T data showing decrease in M at $T \approx 113$ K from the PM state to G-AFM state. (c) Schematic of the measurement circuit. (d) T dependence of the normalized variance of resistance fluctuations ($\langle \Delta R^2 \rangle / \langle R^2 \rangle$) and R.

phase, although its nature and role in the transition is yet to be investigated.

The presence of competing interactions in $Ca_3(Ru_{0.9}Ti_{0.1})_2O_7$ [27] such as intrabilayer ferromagnetic ordering due to itinerant charge carriers and superexchange AFM interactions leads to critical phenomena associated with the transition and the possibility of the coexistence of multiple phases known as phase separation [40].

In this Letter, we probe the collective behavior at the phase transition in $Ca_3(Ru_{0.9}Ti_{0.1})_2O_7$ with low-frequency resistance fluctuations [21,22,26,41–45]. We observe an enhanced noise level across the transition, with a Lorentzian component superimposed on the $1/f^{\alpha}$ background. Our investigation reveals a slowing down of the electron kinetics at the transition, causing a significant rearrangement in the spectral weight distribution of noise. Strong non-Gaussianity observed in the second spectrum of noise suggests glassy kinetics at the transition. The application of B suppresses this non-Gaussianity, indicating the formation of an intermediate spin-glass phase. Our experiment provides unambiguous signatures of the emergent glassy kinetics of electrons across the Mott MIT in $Ca_3(Ru_{0.9}Ti_{0.1})_2O_7$ at finite T.

The T dependence of the resistance (R) while slowly heating the single crystal (sample S1) of $Ca_3(Ru_{0.9}Ti_{0.1})_2O_7$ at 0.5 K/min [Fig. 1(a)] clearly exhibits a metal-to-insulator transition at $T \approx 112$ K, with R increasing by almost five orders of magnitude [see Supplemental Material (SM) Sec. I for device details [46]]. We have indicated three different regions according to the kinks observed in R-T [39]. The crystal has a PM state above 113.5 K [red region, Fig. 1(a)] and a G-type AFM state below 109 K [blue region, Fig. 1(a)]. However, very close to the transition between 109 and 113.5 K [gray region, Fig. 1(a)] the system could be in a mixed phase [Fig. 1(a)]. Figure 1(b) shows a sharp reduction in magnetization (M) when the crystal undergoes a transition from the PM metallic phase to G-AFM insulating phase [39].

Low-frequency $1/f$ noise measurements were performed by capturing four-probe ac voltage fluctuations with a lock-in amplifier, with each block of data being recorded for 40 min with 1000 data points/s, followed by digital signal processing to obtain the power spectral density [PSD, $S_V(f)$, f is the spectral frequency] [Fig. 1(c)] [26,47,48]. The quadratic dependence of $S_V(f)$ with bias across the sample (V) was checked in both metallic and insulating regimes, ensuring that the measurements were performed in the linear Ohmic regime (see SM Sec. II [46]) [49]. The stability of T was maintained within 1 mK, eliminating the fluctuation of T as a possible origin of the excess noise (see SM Sec. III [46]).

The T dependence of the normalized variance of resistance fluctuations, obtained by integrating the PSD over the experimental bandwidth ($f_{\max}$ and $f_{\min}$ are maximum and minimum frequencies, respectively),

$$\frac{\langle \Delta R^2 \rangle}{\langle R^2 \rangle} = \int_{f_{\min}}^{f_{\max}} \frac{S_V(f)}{V^2} df, \tag{1}$$

is shown in Fig. 1(d). We observe a sharp peak in $\langle \Delta R^2 \rangle / \langle R^2 \rangle$ across the transition, where it increases by an order of magnitude. We estimate the phenomenological Hooge parameter, $\gamma_H \approx 10^9$ [50] (see SM Sec. IV [46]). Although in conventional bulk and low-dimensional systems, $\gamma_H \approx 10^{-5}$–1 [41,45,48,49,51–61], such high values have been observed in MIT and attributed to percolation or glassy kinetics [22,24–26,62,63].

To gain a better understanding of the origin of the peak in noise and large γ_H, we performed noise measurements at a more closely spaced T interval of 50 mK, near the transition ($T_c = 111.75$ K). Since the R-T data showed hysteresis with $\Delta T_c \sim 1$–2 K between forward and reverse thermal cycles, we have plotted the data with respect to the shifted temperature $T - T_c$, where T_c is the transition temperature of the corresponding thermal sweep. The representative time (t) dependence of R, close to the transition, is shown in Fig. 2(a) from $T = 111.75$ K (T_c) to $T = 111.45$ K ($T_c - 0.35$ K). It is evident that R fluctuates between high and low states at specific T's. Such two-level fluctuations (TLFs) or random telegraphic noise (RTN) have been observed before in different physical systems such as MOSFETs and perovskite manganites, attributed to the trapping-detrapping of carriers between defect levels and thermally activated switching between coexisting phases [64–67].

Expectedly, at T where TLFs are predominant, we find the noise magnitude to be high and the spectrum deviates strongly from a $1/f^{\alpha}$ nature. Noise measurements in sample S2, taken at a resolution of 20 mK, also show TLFs and similar qualitative data (see SM Secs. V and VI [46]). PSD due to a dynamical process, such as activated fluctuation between two states with a single relaxation time τ_0 and relaxation function $\propto \exp(-t/\tau_0)$, simplifies to a Lorentzian distribution [68]. Hence, we fit the normalized PSD, as shown in Fig. 2(b), with a combination of both $1/f^{\alpha}$ and Lorentzian components, given as [66]

$$\frac{S_V(f)}{V^2} = \frac{A}{f^{\alpha}} + \frac{Bf_c}{f^2 + f_c^2}, \tag{2}$$

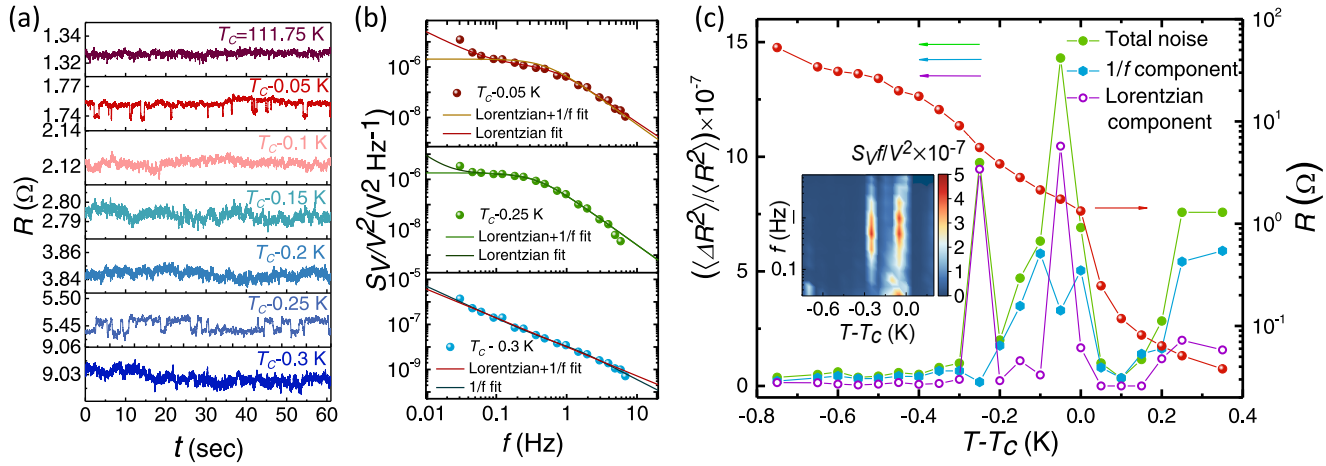

FIG. 2. Noise in $Ca_3(Ru_{0.9}Ti_{0.1})_2O_7$. (a). Resistance ($R$) as a function of time (t) from T_c (111.75 K) to $T_c - 0.3$ K (111.45 K). Two-level fluctuations are observed at $T_c - 0.05$ and $T_c - 0.25$ K. (b) Normalized power spectral density $[S_V(f)/V^2]$ at $T_c - 0.05$, $T_c - 0.25$, and $T_c - 0.3$ K. (c) Dependence of normalized variance $(\langle\Delta R^2\rangle/\langle R^2\rangle)$ and resistance (R) on shifted temperature ($T - T_c$). The inset shows the variation of $S_V f/V^2$ on f and $T - T_c$.

where A and B represent the PSD due to $1/f^\alpha$ and Lorentzian components, respectively, and f_c is the corner frequency corresponding to the relaxation time of the Lorentzian. From the noise spectra shown in Fig. 2(b), it is evident that close to the transition there is a strong Lorentzian component as well as a significant $1/f^\alpha$ background, while away from the transition, $1/f^\alpha$ noise dominates.

The T dependence of $\langle\Delta R^2\rangle/\langle R^2\rangle$ is shown in Fig. 2(c), along with the contributions from the narrow-band Lorentzian and broadband $1/f^\alpha$ component ($\alpha \sim$ 1–1.4; see SM Sec. VII [46]), which have been computed from the fitting parameters of Eq. (2) [66]. We observe two distinct peaks in $\langle\Delta R^2\rangle/\langle R^2\rangle$, at $T = 111.7$ K ($T_c - 0.05$ K) and $T = 111.5$ K ($T_c - 0.25$ K), where the Lorentzian component dominates. The Lorentzian component is maximum around $f_c \approx 0.1$–0.5 Hz [inset of Fig. 2(c)], which is consistent with the fitting parameters (see SM Sec. VII [46]), implying a redistribution of the spectral weight and slowing down of electron kinetics across the transition. The appearance of TLFs in our system is strongly indicative of an emergent collective phase with a long-range correlation that can occur across a phase transition, where the system becomes sensitive to one or very few fluctuators [66,67]. In $Ca_3(Ru_xTi_{1-x})_2O_7$, MIT at T_{MIT} is followed by a magnetic transition at T_N ($T_N > T_{MIT}$) [36] for $x < 0.05$. With increased Ti doping ($x > 0.05$), we observe a single Mott transition as the intermediate metallic phase present at lower doping is unable to form a full percolative network [27], and average transport measurements are unable to resolve the two. However, we find low-frequency noise to be extremely sensitive in resolving the two transitions, with the two distinct peaks in $1/f$ noise, and the appearance of the Lorentzian component at a temperature interval of ∼0.25 K repeatable in multiple samples (see Sec. VI in SM [46]).

To understand the electron kinetics that leads to $1/f^\alpha$ noise across the transition, we further studied the second spectrum [$s^{(2)}(f_2)$, f_2 being its spectral frequency] [69], which is the fourth-order statistics or kurtosis of the voltage noise. $s^{(2)}(f_2)$ is a measure of the correlation or non-Gaussianity of the fluctuations [purple trace in Fig. 3(a)] measured from the integrated noise indicated by $P_i \in [1, N]$ within a bandwidth (f_l, f_H), as evaluated from $S_V(f)$ (see SM Sec. VIII [46]). The non-Gaussian component (NGC) in resistivity fluctuations is an extremely sensitive technique to probe the spectral wandering due to slow charge and spin kinetics, such as those in glasses [52]. In general, NGC indicates two possibilities, (a) percolative network of electrical conduction [26], and (b) long-range correlation between the fluctuators [22,44]. The two cases can be distinguished from the spectral shape as $s^{(2)}(f_2)$ increases at low f_2 for a correlation-induced slowdown because the spectral weight is transferred to lower frequencies, while $s^{(2)}(f_2)$ remains frequency independent in the case of percolation. In our samples, we find $s^{(2)}(f_2) \propto f_2^{-\beta}$ with $\beta \approx 0.2$–0.5 [Fig. 3(b)], at temperatures where the $1/f^\alpha$ component is maximum (at the transition), indicating strong NGC and interactions between the fluctuators. The solid lines [Figs. 3 and 4(b)] represent fits to the data while dashed lines represent the constant background expected for Gaussian fluctuations (see SM Sec. VIII [46]) or uncorrelated fluctuators [26]. The f_2 dependence of $s^{(2)}(f_2)$ eliminates the possibility of additional $1/f^\alpha$ noise arising from classical percolation [70] or dynamical current redistribution (DCR) [71], which can arise at a first-order phase transition owing to the coexistence of phases, since the fluctuators are not correlated in this case. The frequency dependence of $s^{(2)}(f_2)$ indicates that the correlation among P_i, which is a measure of the resistance fluctuations, is nonzero, implying that the fluctuations are related between each time segment. This reveals the presence of "slow" relaxation time in the system, which represents "ergodicity breaking," a possible signature of glassy behavior [72–74] (see SM Secs. VIII and IX [46]).

We repeated the noise measurements at $B = 50$ and 100 mT, applied parallel to the a-b plane, which is higher than the field required to suppress the transition [27,75]. The variation of $\langle\Delta R^2\rangle/\langle R^2\rangle$ with T is shown in Fig. 4(a) ($T_c = 111.5$ K in this thermal cycle). The contributions from the Lorentzian and $1/f^\alpha$ components are computed

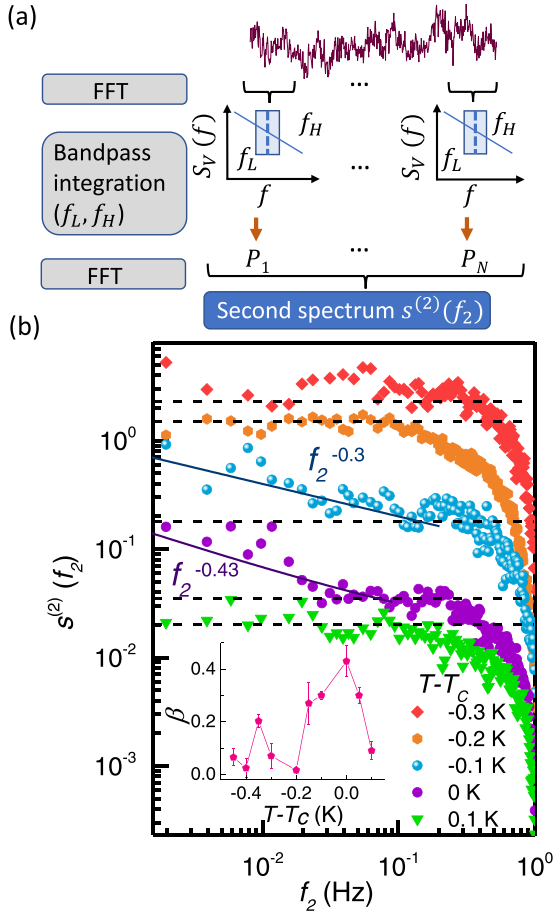

FIG. 3. Non Gaussianity in noise: (a). Schematic of second spectrum analysis. (b). Normalized second spectrum $[s^{(2)}(f_2)]$ at different shifted temperatures $(T - T_c)$, shifted vertically for clarity. Solid lines show the frequency dependence of $s^{(2)}(f_2) \propto f_2^{-\beta}$. Dashed lines are guides to the eye representing a frequency-independent background. The inset shows the variation of exponent β with $T - T_c$.

separately for comparison. We observe complete suppression of the noise peak at lower T while the peak at higher T is partially suppressed. This indicates TLFs to be arising from fluctuators with a magnetic flavor. This can be modeled as fluctuations between two states separated by a finite-energy barrier that is dependent on B. The system can switch between two metastable states with energy E_i and E_v by thermal activation (TA) [67] or by macroscopic quantum tunneling (QMT) [inset of Fig. 4(a)] [76]. Within the framework of this model, a field-dependent energy barrier is given as $E_i(H) = E_0 + \Delta m_i \cdot H$, where $\Delta m_i = m_v - m_i$, m_i and m_v being the magnetic moment associated with the fluctuator in the states i and v, respectively, and H is the applied magnetic field. If E_i changes even slightly, timescales associated with TLFs being exponentially dependent [67,76] also change significantly and go beyond our experimental bandwidth. The peak in noise at lower T possibly arises with the coherent switching of the stripe phase and G-AFM phase corresponding to MIT, while the peak at higher T again comes with the emergence of the PM domain corresponding to Néel transition.

We also analyzed the second spectrum for $B = 50$ and 100 mT at $T - T_c = -0.05$ K where $1/f^\alpha$ noise is maximum

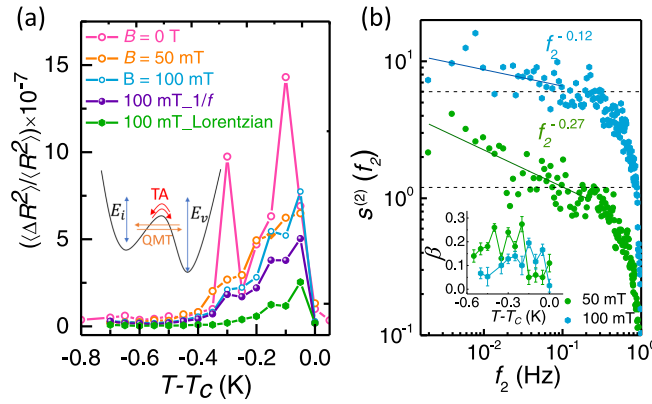

FIG. 4. Magnetic field dependence of noise. (a) Normalized variance $(\langle\Delta R^2\rangle/\langle R^2\rangle)$ as a function of shifted temperature $(T - T_c)$. The inset shows the origin of TLFs across an energy barrier. (b) Normalized second spectrum $[s^{(2)}(f_2)]$ for $B = 100$ and 50 mT at T for maximum β, where $s^{(2)}(f_2) \propto f_2^{-\beta}$ shown by solid lines. The inset shows the variation of β with $T - T_c$.

[Fig. 4(b)]. Crucially, we observe that compared to the $B = 0$ case, the variation of $s^{(2)}(f_2)$ with f_2 is progressively weakened, as B is increased from 50 to 100 mT, with β varying between 0.05 and 0.3 in the entire T range [inset of Fig. 4(b)]. We observe a similar suppression for different thermal cycles (see SM Sec. X [46]), thereby strongly indicating the formation of a spin-glass state near the transition.

Glassy electron kinetics, usually attributed to geometric frustration and quenched disorder, has been investigated close to MIT [20,20,22,77,78]. We report an emerging spin-glass state near a first-order Mott MIT [27] at a high T of ≈110 K without any geometric frustration in the system. The emergence of such a glassy state is not manifested in the R-T of the sample (see SM Sec. XI [46]). Several possibilities of the origin of spin-glass formation exist. In the case of RP materials such as Sr_3MnTiO_7, the structural distortion of MO_6 octahedra, and the random distribution of Mn^3/Mn^{4+} might be responsible for the observed spin-glass behavior [79]. In $Ca_4Mn_3O_{10}$, weak ferromagnetic clusters can arise from inhomogeneously distributed distortions of the crystallographic structure [80]. A spin-glass phase has been predicted theoretically in $PrAu_2Si_2$ [81], which represents a system to achieve frustration with neither static disorder nor geometrically frustrated lattices, but through competing long-range interactions. We believe in our case, spin-glass behavior can appear due to the distortion of the RuO_6 octahedra due to the addition of Ti atoms as well as the presence of trace amounts of magnetic defects such as Ru^{3+}/Ru^{5+}. Such defects have been shown to give rise to a spin-glass state in double perovskite ruthenates [82]. Another possibility is the frustration of competing interactions which gives rise to a self-generated glass phase [83]. Further investigation is necessary in this regard.

In conclusion, we have probed the Mott transition in $Ca_3(Ru_{0.9}Ti_{0.1})_2O_7$ with low-frequency noise. We observe an increase in $1/f^\alpha$ noise by an order of magnitude across the transition. These slow fluctuation timescales originate from the glassy kinetics of the electrons close to the MIT, which is

verified by the frequency dependence of the second spectrum. Magnetic field-dependent measurements indicate towards an intermittent spin-glass formation across a first-order Mott MIT.

S.K. acknowledges PMRF, and S.I. and A.G. acknowledge MeitY for support. Z.Q.M. and Y.W. acknowledge support of U.S. NSF through the Penn State 2DCC-MIP under NSF Cooperative Agreement No. DMR-2039351.

[1] N. F. Mott, Proc. Phys. Soc. A **62**, 416 (1949).
[2] N. F. Mott, Rev. Mod. Phys. **40**, 677 (1968).
[3] M. Imada, A. Fujimori, and Y. Tokura, Rev. Mod. Phys. **70**, 1039 (1998).
[4] C.-M. Jian, Z. Bi, and C. Xu, Phys. Rev. B **96**, 115122 (2017).
[5] T. Furukawa, K. Miyagawa, H. Taniguchi, R. Kato, and K. Kanoda, Nat. Phys. **11**, 221 (2015).
[6] H. Terletska, J. Vučičević, D. Tanasković, and V. Dobrosavljević, Phys. Rev. Lett. **107**, 026401 (2011).
[7] T. Li, S. Jiang, L. Li, Y. Zhang, K. Kang, J. Zhu, K. Watanabe, T. Taniguchi, D. Chowdhury, L. Fu *et al.*, Nature (London) **597**, 350 (2021).
[8] P. Salev, L. Fratino, D. Sasaki, R. Berkoun, J. Del Valle, Y. Kalcheim, Y. Takamura, M. Rozenberg, and I. K. Schuller, Nat. Commun. **12**, 5499 (2021).
[9] S. Hormoz and S. Ramanathan, Solid-State Electron. **54**, 654 (2010).
[10] S. B. Roy, *Mott Insulators* (IOP Publishing, 2019).
[11] S. Iqbal, L. T. Duy, H. Kang, R. Singh, M. Kumar, J. Park, and H. Seo, Adv. Funct. Mater. **31**, 2102567 (2021).
[12] Y. Wang, K.-M. Kang, M. Kim, H.-S. Lee, R. Waser, D. Wouters, R. Dittmann, J. J. Yang, and H.-H. Park, Mater. Today **28**, 63 (2019).
[13] S. Zhang and G. Galli, npj Comput. Mater. **6**, 1 (2020).
[14] E. Abrahams, *50 Years of Anderson Localization*, International Journal of Modern Physics Vol. 24, Pt. 1 (World Scientific, Singapore, 2010).
[15] N. Mott, *Metal-Insulator Transitions* (CRC Press, 2004).
[16] B. Spivak, S. V. Kravchenko, S. A. Kivelson, and X. P. A. Gao, Rev. Mod. Phys. **82**, 1743 (2010).
[17] E. Dagotto, Science **309**, 257 (2005).
[18] Y. Tokura and N. Nagaosa, Science **288**, 462 (2000).
[19] A. Hewson, *The Kondo Problem to Heavy Fermions*, Cambridge Studies in Magnetism (Cambridge University Press, Cambridge, UK, 1997).
[20] V. Dobrosavljević, D. Tanasković, and A. A. Pastor, Phys. Rev. Lett. **90**, 016402 (2003).
[21] B. Hartmann, D. Zielke, J. Polzin, T. Sasaki, and J. Müller, Phys. Rev. Lett. **114**, 216403 (2015).
[22] S. Kar, A. K. Raychaudhuri, A. Ghosh, H. V. Löhneysen, and G. Weiss, Phys. Rev. Lett. **91**, 216603 (2003).
[23] S. c. v. Bogdanovich and D. Popović, Phys. Rev. Lett. **88**, 236401 (2002).
[24] Z. Topalian, S.-Y. Li, G. A. Niklasson, C. G. Granqvist, and L. B. Kish, J. Appl. Phys. **117**, 025303 (2015).
[25] V. Podzorov, M. Uehara, M. E. Gershenson, T. Y. Koo, and S.-W. Cheong, Phys. Rev. B **61**, R3784 (2000).
[26] A. Sahoo, S. D. Ha, S. Ramanathan, and A. Ghosh, Phys. Rev. B **90**, 085116 (2014).
[27] J. Peng, X. Ke, G. Wang, J. E. Ortmann, D. Fobes, T. Hong, W. Tian, X. Wu, and Z. Q. Mao, Phys. Rev. B **87**, 085125 (2013).
[28] I. B. Sharma and D. Singh, Bull. Mater. Sci. **21**, 363 (1998).
[29] Y. Maeno, H. Hashimoto, K. Yoshida, S. Nishizaki, T. Fujita, J. G. Bednorz, and F. Lichtenberg, Nature (London) **372**, 532 (1994).
[30] A. J. Leggett and Y. Liu, J. Supercond. Novel Magn. **34**, 1647 (2021).
[31] S. A. Grigera, R. S. Perry, A. J. Schofield, M. Chiao, S. R. Julian, G. G. Lonzarich, S. I. Ikeda, Y. Maeno, A. J. Millis, and A. P. Mackenzie, Science **294**, 329 (2001).
[32] S. Nakatsuji, D. Hall, L. Balicas, Z. Fisk, K. Sugahara, M. Yoshioka, and Y. Maeno, Phys. Rev. Lett. **90**, 137202 (2003).
[33] J. M. Longo, P. M. Raccah, and J. B. Goodenough, Nature (London) **39**, 1327 (1968).
[34] S. Nakatsuji, S.-i. Ikeda, and Y. Maeno, J. Phys. Soc. Jpn. **66**, 1868 (1997).
[35] T. He and R. J. Cava, Phys. Rev. B **63**, 172403 (2001).
[36] G. Cao, S. McCall, J. E. Crow, and R. P. Guertin, Phys. Rev. Lett. **78**, 1751 (1997).
[37] F. Baumberger, N. J. C. Ingle, N. Kikugawa, M. A. Hossain, W. Meevasana, R. S. Perry, K. M. Shen, D. H. Lu, A. Damascelli, A. Rost, A. P. Mackenzie, Z. Hussain, and Z.-X. Shen, Phys. Rev. Lett. **96**, 107601 (2006).
[38] X. Ke, J. Peng, D. J. Singh, T. Hong, W. Tian, C. R. Dela Cruz, and Z. Q. Mao, Phys. Rev. B **84**, 201102(R) (2011).
[39] A. Gangshettiwar, Y. Zhu, Z. Jiang, J. Peng, Y. Wang, J. He, J. Zhou, Z. Mao, and K. Lai, Phys. Rev. B **101**, 201106(R) (2020).
[40] P. G. Radaelli, R. M. Ibberson, D. N. Argyriou, H. Casalta, K. H. Andersen, S.-W. Cheong, and J. F. Mitchell, Phys. Rev. B **63**, 172419 (2001).
[41] P. Dutta and P. M. Horn, Rev. Mod. Phys. **53**, 497 (1981).
[42] H. K. Kundu, S. Ray, K. Dolui, V. Bagwe, P. R. Choudhury, S. B. Krupanidhi, T. Das, P. Raychaudhuri, and A. Bid, Phys. Rev. Lett. **119**, 226802 (2017).
[43] S. Kundu, T. Bar, R. K. Nayak, and B. Bansal, Phys. Rev. Lett. **124**, 095703 (2020).
[44] U. Chandni, A. Ghosh, H. S. Vijaya, and S. Mohan, Phys. Rev. Lett. **102**, 025701 (2009).
[45] S. Islam, S. Shamim, and A. Ghosh, Adv. Mater., 2109671 (2022).
[46] See Supplemental Material at http://link.aps.org/supplemental/10.1103/PhysRevB.106.L201112 for device details; power spectral density with bias; temperature fluctuation noise; estimation of Hooge parameter; two-level fluctuations; noise measurements in sample S2; variation of fit parameters of power spectral density with temperature; second spectrum; second spectrum and glassy behavior in sample S2; second spectrum of second thermal cycle of sample S1; and resistance versus temperature in magnetic field.
[47] A. Ghosh, S. Kar, A. Bid, and A. Raychaudhuri, arXiv:cond-mat/0402130.

[48] S. Bhattacharyya, M. Banerjee, H. Nhalil, S. Islam, C. Dasgupta, S. Elizabeth, and A. Ghosh, ACS Nano **9**, 12529 (2015).
[49] S. Islam, S. Bhattacharyya, A. Kandala, A. Richardella, N. Samarth, and A. Ghosh, Appl. Phys. Lett. **111**, 062107 (2017).
[50] F. Hooge, Phys. Lett. A **29**, 139 (1969).
[51] J. H. Scofield, J. V. Mantese, and W. W. Webb, Phys. Rev. B **32**, 736 (1985).
[52] M. B. Weissman, Rev. Mod. Phys. **60**, 537 (1988).
[53] A. N. Pal and A. Ghosh, Appl. Phys. Lett. **95**, 082105 (2009).
[54] V. K. Sangwan, H. N. Arnold, D. Jariwala, T. J. Marks, L. J. Lauhon, and M. C. Hersam, Nano Lett. **13**, 4351 (2013).
[55] A. N. Pal, S. Ghatak, V. Kochat, E. S. Sneha, A. Sampathkumar, S. Raghavan, and A. Ghosh, ACS Nano **5**, 2075 (2011).
[56] P. Karnatak, T. P. Sai, S. Goswami, S. Ghatak, S. Kaushal, and A. Ghosh, Nat. Commun. **7**, 13703 (2016).
[57] S. Kakkar, P. Karnatak, M. A. Aamir, K. Watanabe, T. Taniguchi, and A. Ghosh, Nanoscale **12**, 17762 (2020).
[58] P. Karnatak, T. Paul, S. Islam, and A. Ghosh, Adv. Phys.: X **2**, 428 (2017).
[59] S. Shamim, S. Mahapatra, C. Polley, M. Y. Simmons, and A. Ghosh, Phys. Rev. B **83**, 233304 (2011).
[60] A. N. Pal and A. Ghosh, Phys. Rev. Lett. **102**, 126805 (2009).
[61] A. Ghosh and A. K. Raychaudhuri, Phys. Rev. Lett. **84**, 4681 (2000).
[62] O. Cohen and Z. Ovadyahu, Phys. Rev. B **50**, 10442 (1994).
[63] B. R. Conrad, W. G. Cullen, W. Yan, and E. D. Williams, Appl. Phys. Lett. **91**, 242110 (2007).
[64] Z. Li, M. Sotto, F. Liu, M. K. Husain, H. Yoshimoto, Y. Sasago, D. Hisamoto, I. Tomita, Y. Tsuchiya, and S. Saito, Sci. Rep. **8**, 1 (2018).
[65] X. Li, T. Zanotti, T. Wang, K. Zhu, F. M. Puglisi, and M. Lanza, Adv. Funct. Mater. **31**, 2102172 (2021).
[66] A. Bid, A. Guha, and A. K. Raychaudhuri, Phys. Rev. B **67**, 174415 (2003).
[67] B. Raquet, A. Anane, S. Wirth, P. Xiong, and S. von Molnár, Phys. Rev. Lett. **84**, 4485 (2000).
[68] P. Dutta, P. Dimon, and P. M. Horn, Phys. Rev. Lett. **43**, 646 (1979).
[69] G. T. Seidler and S. A. Solin, Phys. Rev. B **53**, 9753 (1996).
[70] R. H. Koch, R. B. Laibowitz, E. I. Alessandrini, and J. M. Viggiano, Phys. Rev. B **32**, 6932 (1985).
[71] G. T. Seidler, S. A. Solin, and A. C. Marley, Phys. Rev. Lett. **76**, 3049 (1996).
[72] Z. Kutnjak, C. Filipič, R. Pirc, A. Levstik, R. Farhi, and M. El Marssi, Phys. Rev. B **59**, 294 (1999).
[73] L. F. Cugliandolo, J. Kurchan, P. Le Doussal, and L. Peliti, Phys. Rev. Lett. **78**, 350 (1997).
[74] G. Carleo, F. Becca, M. Schiró, and M. Fabrizio, Sci. Rep. **2**, 243 (2012).
[75] M. Zhu, J. Peng, T. Zou, K. Prokes, S. D. Mahanti, T. Hong, Z. Q. Mao, G. Q. Liu, and X. Ke, Phys. Rev. Lett. **116**, 216401 (2016).
[76] L.-D. Chang and S. Chakravarty, Phys. Rev. B **29**, 130 (1984).
[77] J. Jaroszyński, D. Popović, and T. Klapwijk, Phys. E **12**, 612 (2002).
[78] J. Brandenburg, J. Müller, and J. A. Schlueter, New J. Phys. **14**, 023033 (2012).
[79] T. Nan, S. Emori, C. T. Boone, X. Wang, T. M. Oxholm, J. G. Jones, B. M. Howe, G. J. Brown, and N. X. Sun, Phys. Rev. B **91**, 214416 (2015).
[80] J. Lago, P. D. Battle, and M. J. Rosseinsky, J. Phys.: Condens. Matter **12**, 2505 (2000).
[81] E. Goremychkin, R. Osborn, B. Rainford, R. Macaluso, D. Adroja, and M. Koza, Nat. Phys. **4**, 766 (2008).
[82] H. Yatsuzuka, Y. Haraguchi, A. Matsuo, K. Kindo, and H. A. Katori, Sci. Rep. **12**, 2429 (2022).
[83] J. Schmalian and P. G. Wolynes, Phys. Rev. Lett. **85**, 836 (2000).

Correction: The "Corresponding author" identifier was removed from the byline footnote for the second author during the proof production process and has been restored.